Analysis and modelling of non-equilibrium sorption of aromatic micro-pollutants on GAC with a multi-compartment dynamic model

Geoffroy Lesage, Mathieu Sperandio, Ligia Tiruta-Barna

Title: Analysis and modelling of non-equilibrium sorption of aromatic micro-pollutants on GAC with a multi-compartment dynamic model

Authors: Geoffroy Lesage, Mathieu Sperandio, Ligia Tiruta-Barna

PII: S1385-8947(10)00264-0
DOI: doi:10.1016/j.cej.2010.03.045
Reference: CEJ 6885

To appear in: *Chemical Engineering Journal*

Received date: 18-9-2009
Revised date: 18-3-2010
Accepted date: 19-3-2010

Please cite this article as: G. Lesage, M. Sperandio, L. Tiruta-Barna, Analysis and modelling of non-equilibrium sorption of aromatic micro-pollutants on GAC with a multi-compartment dynamic model, *Chemical Engineering Journal* (2008), doi:10.1016/j.cej.2010.03.045

Analysis and modelling of non-equilibrium sorption of aromatic micro-pollutants on GAC with a multi-compartment dynamic model

GEOFFROY LESAGE, MATHIEU SPERANDIO AND LIGIA TIRUTA-BARNA*

Université de Toulouse; INSA, UPS, INP; LISBP, 135 Avenue de Rangueil, F-31077 Toulouse, France

INRA, UMR792, Laboratoire d'Ingénierie des Systèmes Biologiques et des Procédés, F-31400 Toulouse, France

CNRS, UMR5504, F-31400 Toulouse, France;*

Abstract

The optimisation of granular activated carbon (GAC) processes for industrial wastewater treatment requires the development of dynamic model that considers adsorption in multi-compartment porous media. In this work, the adsorption of toluene and naphthalene on GAC is investigated. Sorption equilibrium and kinetic experiments were performed at laboratory scale using low contaminant concentrations. The experimental conditions were chosen so as to simultaneously explore the different ranges of concentrations typically encountered in industrial wastewaters. The sorption behaviour was then explained through modelling taking into account the main equilibrium and transport phenomena and three adsorption compartments: the GAC particle surface, the macro- and meso-pores, and the micropores. The pore diffusion and solid diffusion were both considered to be coupled with a linear adsorption isotherm. With one set of four parameters adjusted for an adsorbent/contaminant pair, the model satisfactorily describes the non-equilibrium adsorption/desorption processes in different operating conditions and initial conditions.

Keywords: *Kinetics, Mass transfer, Diffusion, PAH, Toluene.*

* Corresponding author. Tel: +33(0)5 61 55 97 88; Fax: +33 (0)5 61 55 97 60
E-mail address: ligia.barna@insa-toulouse.fr

1. Introduction

Because of industrial and urban development, many hazardous organic substances and micro-pollutants are discharged into the environment via wastewaters (Williams, 1990; Douben, 2003). Removing chemical contaminants from wastewaters continues to be a central problem in environmental remediation and severe discharge constraints are now imposed by legislation for a number of chemicals (Water Framework Directive 2000) like monoaromatic and polyaromatic hydrocarbons. Adsorption is a well established technique for the removal of low concentrations of organic pollutants from industrial wastewater. Among the many adsorbents available, activated carbon is effective in removing a large variety of organic components (Seidel et al., 1985). Treatment options may range from activated carbons that differ in pore structure and surface chemistry to the control of one or more chemical compounds and mixtures. Granular Activated Carbon (GAC) has been shown to be efficient for the removal of organic micropollutants including aromatic hydrocarbons, halogenated hydrocarbons, pesticides, polychlorobiphenyl and surfactants (Zimmerman et al., 2004). The optimisation of GAC processes for industrial wastewater treatment demands a good knowledge of the adsorption and desorption dynamics. When GAC is operated in a completely mixed reactor (ref) fed with wastewater, it can be subjected to micropollutant concentrations that vary with time, leading to non-equilibrium in the system. Few studies have reported the analysis of this dynamics, which depends on mechanisms of internal diffusion into GAC in different compartments of the granular medium: surface, macro-porosity and micro-porosity.

The present work focuses on two substances typically found in industrial wastewaters: toluene and naphthalene. Toluene and naphthalene have been characterized as potential human carcinogens and their maximum permissible concentrations in drinking water range from 4.6 to 0.3μg L^{-1} among different countries (WHO, 2006). Toluene is a very popular solvent, used in the electronics, chemical and printing industries. Polycyclic aromatic hydrocarbons (PAH) are produced by human activity, chiefly in the pyrolysis and combustion processes employed in industry, transport and heating (Bouchez et al., 1996). These substances cause severe environmental pollution because of their persistence in the environment and their genotoxicity to living organisms. The chemical properties of toluene and naphthalene differ by their volatility and hydrophobicity: toluene is a highly volatile organic compound (VOC) while naphthalene is characterized by lower water solubility and high octanol-water partioning coefficients (Log K_{ow}). Naphthalene is one of the most soluble of the PAH and therefore represents the worst case for PAH mobility. In many studies, naphthalene is used as a model chemical for hydrophobic organics. Since GAC is a heterogeneous granular medium with particle sizes ranging from 0.5 to 10 mm, a bimodal pore distribution (macro and microporous) and a high specific surface area (500-2000m^2 g^{-1}) (Cheremisinoff and Cheremisinoff, 1993), it is particularly suitable for the efficient sorption of high molecular weight organic molecules with lipophilic properties, as is the case with PAH (Jonker and Koelmans, 2002). Ania et al. (2007) found that the adsorption of naphthalene depended strongly on the pore size distribution of the adsorbent, particularly narrow microporosity. Although the microporous surface constitutes a major fraction of the specific surface area, adsorption of organic micropollutants also occurs on the external surface of particles and macro-pore walls. Whereas the experimental characterisation of

adsorption of GAC is frequent in the literature (Seredych et al., 2005; Ania et al., 2007; Valderrama et al., 2007; 2008a; 2008b; Cabal et al., 2009b), dynamic models that consider adsorption in multi-compartment porous media are rare. The sorption of organic micropollutants onto natural and synthetic sorbents has been described as a complex process in which the properties of the sorbate and the solvent play a critical role. The sorption process occurs within the boundary layer around the sorbent and proceeds in the liquid-filled pores or along the walls of the pores of the sorbent. As the classical modelling approaches point out, the adsorption process is composed of several steps:

- Diffusion of the pollutant from bulk liquid through the thin film of liquid surrounding the GAC particle (external transfer).
- Pollutant adsorption on the particle's external surface.
- Diffusion inside the pores (internal transfer) by two main mechanisms: pore diffusion (in large pores) and/or surface diffusion (in all pores, particularly in narrow, molecular-size-like pores).
- Adsorption on the pore walls.

Within a perfectly stirred reactor at constant temperature, adsorption rate is controlled by extra- or intra-particular diffusion steps. The relative importance of these steps depends on the adsorbent structure (particle diameter, pore length and diameter), solute properties (solute diffusivities) and hydrodynamic conditions. The design of a full-scale process requires knowledge not only of the equilibrium state but also of the dynamics of the solute adsorption/desorption processes, which depend strongly on the different steps described above.

In most studies, the adsorption rate of organic compounds from aqueous solutions is modelled by using several simplistic mathematical expressions that include the pseudo-first order (Lagergren, 1898), pseudo–second order (Vinod and Anirudhan, 2003; Wu et al., 2009), the intraparticle diffusion model (Weber, 1963; Cabal et al., 2009a) and the Elovich model (Chien and Clayton, 1980). Although these kinetic equations have been frequently employed to interpret adsorption data obtained under non-equilibrium conditions, their theoretical origins still remain unknown (Liu and Shen, 2008). The specific parameters contained in these equations can be determined only by fitting on experimental data and are dependent on the operating conditions, e.g. the initial sorbate concentrations. Wu et al (2009) observed that, for the same sorbate/sorbent pair, the performance of a given kinetic model depended on the particle sizes. Another common aspect of most studies on PAH adsorption is that the solutions used were relatively concentrated (with respect to the PAH solubility) and prepared using a co-solvent (alcohol), in a narrow range of concentration values.

To describe the equilibrium adsorption, the most commonly used models are the Langmuir and Freundlich models (Cornelissen et al., 2005; Pikaar et al., 2006). Pikaar et al. (2006) have performed a statistical analysis on isotherm models to fit sorption data for the sorption of organic compounds to activated carbon and found that the dual Langmuir equation is, in general, preferable to the single and triple Langmuir equations, the Freundlich equation, a Polanyi-Dubinin-Manes equation, or the Toth equation. Naphthalene adsorption equilibrium in aqueous solution has been studied through the Langmuir-Freundlich single solute isotherm (Derylo-Marczewska, 1984; Ania et al., 2007)

123 However, few works have developed physical deterministic models for the
124 explanation of the adsorption kinetics of toluene and naphthalene on activated
125 carbon. Some studies have been conducted on simulation and prediction of pilot
126 plant and full-scale adsorber data, e.g. Crittenden et al. (1987), who used a
127 homogeneous solid diffusion model (HDSM) of GAC adsorption of dichloroethylene
128 in a contaminated groundwater matrix. Valderrama et al. (2008a), have studied PAH
129 removal through GAC adsorption and found that the rate-determining step of PAH
130 extraction is the sorbent-phase diffusion. They used two non-equilibrium adsorption
131 models: the Homogeneous Particle Diffusion Model (HPDM) and the Shell
132 Progressive Model (SPM) and have determined PAH effective particle diffusion
133 coefficients (D_{eff}) in the range $1.1*10^{-13}$–$6.0*10^{-14}$ $m^2.s^{-1}$. Though many papers
134 dealing with adsorption of organic substances from aqueous solutions have been
135 published (Seredych et al., 2005; Ania et al., 2007; Valderrama et al., 2007; 2008a;
136 2008b; Cabal et al., 2009b); the rate and the mechanisms of the adsorption process
137 itself remain unclear. Therefore, it would be appropriate to evaluate a model capable
138 of predicting the equilibrium and kinetic sorption performance of GAC for aqueous
139 trace organic molecules based on fundamental sorbent and sorbate properties.
140
141 Therefore, in this paper, aromatics with one and two rings (toluene and naphthalene)
142 are evaluated in a set of sorption and desorption tests on GAC in completely stirred
143 cells, with the following objectives:
144 - to determine the adsorption behaviour, i.e. kinetic and equilibrium parameters, on
145 an extended time scale (short term to long term), in extreme concentration conditions
146 (low to high) expected to be found in ground and industrial wastewater, i.e. typically
147 in the range of 0.2–200g m^{-3},

- to quantify the main phenomena through a mechanistic modelling approach,
- and to build a model containing a reduced number of adjusted parameters (parameters with a physical meaning) which simulates the adsorption/desorption behaviour in different operating conditions. This model should be easy to handle and resolve and should also allow for its integration in larger models of more complex systems (for example adsorber modelling, or coupling with other bio-physicochemical phenomena).

2. Materials and experimental methods

Adsorbates and adsorbents

Toluene and naphthalene were supplied by Sigma Aldrich. Toluene from the BTEX group solvents was chosen as a typical mono-aromatic hydrocarbon, naphthalene was chosen as a model compound for a light molecule of the group of polyaromatic hydrocarbons. All the above chemicals were more than 99% pure. Organic stock solutions were prepared in ultrapure water in a concentration range of approximately 0.2 to 200g m^{-3}.

The Granular Activated Carbon (GAC) employed as the adsorbent was supplied by Pica and had the characteristics presented in Table 2. The GAC was obtained from coconut which was thermally activated and had a mean granulometry of 0.5-0.8mm. The BET (Brunauer–Emmett–Teller) surface area (1707m^2 g^{-1}) was obtained from N_2 adsorption isotherms at 77K on an ASAP2010 micrometrics apparatus. The isotherms were used to calculate the total pore volume, specific surface area and pore size distributions with t-plot and HK (Horwath-Kawazoe) modelling. Prior to

addition to the vials, the GAC was rinsed three times with ultra-pure water to remove dissolved contaminants and fine particles, which could have affected the adsorption capacity of the activated carbon (Summers and Roberts, 1988; Srivastava and Tyagi, 1995). The GAC was then dried at 105°C for 24h prior to storage in a dessicator until use (Cooney and Xi, 1994). It is generally accepted that activated carbon has a bimodal pore size distribution and contains pores ranging from several microns to a few angstroms. According to the classification by the International Union of Pure and Analytical Chemistry (IUPAC), there are three types of pores: micropores having dimensions less than 2nm, macropores larger than 500nm, and mesopores lying between these two limits.

Adsorption of pollutants on GAC

Adsorption measurements of toluene and naphthalene from aqueous solutions on carbon adsorbents were performed at 25°C in a stirred batch system, which consisted of 120mL amber glass vials filled without headspace and closed with Teflon-coated septa. Experiments were conducted in laboratory ultrapure water (tap water treated by ion exchange and UV). All points were obtained in duplicate or triplicate. A control sample without GAC was identically prepared for each experiment. The different aqueous solutions of pollutants without solid were first stirred on a rotary stirrer for 72h. Measurement by GCMS determined the real initial concentration of the solution before the adsorption experiment, taking into account the artefacts associated with the adsorption of pollutants on the different components of the reactor (Huang et al., 1988). The GAC was then weighed with an accuracy of +/- 0.001g and added into the vials. Tightly closed, the vials were shaken for 2-168h for the kinetic study. This revealed that the concentration values stabilised

198 (suggesting that equilibrium was reached) in 15h for NAP and 24h for Toluene (see
199 below). After stirring, the tubes were centrifuged for 20min at 2500rpm. The residual
200 pollutant concentration of the supernatant was then determined by GCMS analysis
201 and the adsorbed amount was calculated from the difference between initial and
202 residual concentrations. The adsorbed quantity Q_{exp} is given by the following
203 equation:

204 $$Q_{exp} = (C_{0,exp} - C_{exp}).\frac{V}{S}, \quad (1)$$

205 Where $C_{0,exp}$ and C_{exp} are the initial and equilibrium concentrations respectively
206 (g m^{-3}), V the volume of solution (m^3) and S the mass of solid (g).

207

208 *Analytical procedures*

209 Pollutant concentrations were determined using a gas chromatograph (Varian 3900),
210 equipped with a mass spectrometer detector (Saturn 2100T) using helium (99.999%
211 purity) as carrier gas coupled with an automatic headspace sampler (Quma HSS40).
212 Separation was accomplished using a 30m*0.25mm*0.25µm column (fused silica
213 VARIAN, type VF-5MS (5% phenyl 95% dimethylpolysiloxane)). The water samples
214 (10mL) were transferred to 20mL glass vials with Teflon-coated septa and aluminium
215 seals. The samples were equilibrated for 30min at 80°C and an aliquot of 1mL of the
216 headspace gas was injected into the gas chromatograph. The detection limit was
217 1µg L^{-1}. The accuracy for measurements of split samples containing a concentration
218 of 1.5µg L^{-1} was +/- 0.1µg L^{-1}. All vials were first washed and dried in a 500°C oven to
219 remove all traces of organics.

220

221

222

SEM analysis

A JEOL 5410LV Scanning Electron Microscope was used to observe the surface morphology of GAC (Figure 1.a). Prior to analysis, samples were dried in a vacuum oven at room temperature and then gold coated.

3. Modelling

The model applied was based on the four-step conceptual model:

- External diffusion of the pollutant through the thin liquid film surrounding the GAC particle.
- Pollutant adsorption on the particle's external surface.
- Internal diffusion by two main mechanisms: pore diffusion (in large pores) and surface diffusion.
- Adsorption on the pore walls.

And on the following supplementary assumptions:

- The adsorbent particles are spherical (particle diameter is given by the arithmetic mean value of the mesh size) (Figure 1.b).
- Pores of different sizes are parallel, i.e. transfer between different types of pore is not considered.
- Two main diffusion mechanisms should be taken into account. For large pores (macro- and meso-pores) only the pore diffusion is considered because it is several orders of magnitude faster than the solid diffusion. As the two mechanisms occur in parallel, the slower one can be ignored. For the narrow (micro) pores, only solid diffusion is considered.

- Two pore categories are considered: 1) macropores (the ratio of volume to surface area is very small for the macropores of the adsorbent studied); 2) micropores (pore size < 2nm).

Consequently, the model contains three adsorption compartments: the external surface, the macro/meso pores and the micropore surfaces.

The external transfer is characterised by:

- the specific surface area a_s ($m^2\ m^{-3}$) corresponding to the geometric surface area of the particles of radius R (m),
- the external mass transfer coefficient k_{ext} ($m\ s^{-1}$) associated with this surface.

According to the principles stated above, the dynamic adsorption model was composed of the following equations.

-Macro- and meso-pore diffusion and adsorption (in spherical coordinates):

$$\varepsilon_p \frac{\partial C_p}{\partial t} + \sigma_p \rho \frac{\partial Q_p}{\partial t} = \frac{1}{r^2} \frac{\partial}{\partial r}\left(r^2 D_e \frac{\partial C_p}{\partial r} \right) \quad (2)$$

with the boundary conditions:

- r=0, $\frac{\partial C_p}{\partial r} = 0$ (3)

- r=R, $D_e \frac{\partial C_p}{\partial r} = k_{ext}(C - C_p|_R) \equiv flux_p$ (4)

C is the bulk concentration ($g\ m^{-3}$). For the meso- and macro-pore compartment: C_p and Q_p are the pore concentration ($g\ m^{-3}$) and adsorbed quantity ($g\ m^{-2}$) at local coordinates of time t (s) and space r (m), D_e is the effective diffusion coefficient ($m^2\ s^{-1}$), ε_p is the porosity, ρ ($g\ m^{-3}$) is the particle density, σ_p is the specific surface area ($m^2\ g^{-1}$), $flux_p$ ($g\ m^{-2} s^{-1}$) is the flux exchanged between the pore compartment and the bulk liquid phase.

-Micropores (pore width comparable with the molecular size) solid diffusion

$$\frac{\partial Q_{mp}}{\partial t} = \frac{1}{r^2}\frac{\partial}{\partial r}\left(r^2 D_s \frac{\partial Q_{mp}}{\partial r} \right) \quad (5)$$

with the boundary conditions:

- r=0, $\frac{\partial Q_{mp}}{\partial r} = 0$ (6)

- r=R, $D_s \frac{\partial Q_{mp}}{\partial r} = \frac{k_{ext}}{\sigma_{mp}\rho}(C - C^e_{mp}\big|_R)$ (7)

The flux exchanged between the micropores and the bulk liquid is:

$$k_{ext}(C - C^e_{mp}\big|_R) \equiv flux_{mp} \quad (8)$$

For the micropore compartment (subscript mp): Q_{mp} is the locally adsorbed quantity (g m^{-2}), $C^e_{mp}\big|_R$ is the concentration at R in equilibrium with Q_{mp} at R, D_s is the surface diffusion coefficient (m^2 s^{-1}), σ_{mp} is the specific surface area (m^2 g^{-1}), $flux_{mp}$ (g $m^{-2}s^{-1}$) is the flux exchanged between the micropore compartment and the bulk liquid.

-External transfer and surface adsorption:

$$\frac{dQ_{ext}}{dt} = k_{ext}(C - C^e_{ext})\frac{a_s}{\sigma_{ext}\rho} \quad (9)$$

$$k_{ext}(C - C^e_{ext}) \equiv flux_{ext} \quad (10)$$

Q_{ext} is the quantity adsorbed (g m^{-2}) on the external surface of particles (variable only in time), C^e_{ext} is the liquid film concentration near the particle side in equilibrium with Q_{ext}, σ_{ext} is the external specific area available for adsorption (m^2 g^{-1}), $flux_{ext}$ (g $m^{-2}s^{-1}$) is the flux exchanged between the particle external surface and the bulk liquid.

-Bulk liquid mass balance:

The variation of pollutant concentration in the bulk liquid is due to the pollutant fluxes transferred towards the particle's external surface and to the pores.

$$\varepsilon \frac{dC}{dt} = -(a_s flux_{ext} + a_s flux_p + a_s flux_{mp}) \quad (11)$$

The adsorption isotherm is taken to be linear for the concentration range limited by the weak solubility. Saturation was not observed in any set of experiments. The adsorption constant K_e is expressed in $m^3\ m^{-2}$ and represents a partition coefficient between the liquid and the surface. Adsorption is also considered to be rapid and reversible while a physical interaction mechanism is involved; the local equilibrium assumption is adopted in the model. The same linear adsorption equation was applied for all compartments, for example in the macro and mesopores:

$$Q_p = K_e C_p \quad (12)$$

$$\frac{dQ_p}{dt} = K_e \frac{dC_p}{dt} \quad (13)$$

The disadvantage of the present model with respect to its resolution and practical applications is the presence of two-dimensional variables C_p, Q_p and Q_{mp} (time and radius). Previous modelling studies of adsorption systems (Do and Rice, 1986; Goto et al., 1990) revealed the possibility of transforming the models based on partial differential equations (time and space) into simple differential equations (time) in the case of linear absorption, for both pore diffusion and solid diffusion mechanisms.

In this simplified approach, mean concentrations are used instead of the radially varying concentrations. One of the consequences is the possibility of using the "linear driving force" model (Gleuckauf, 1947) associated with a global mass transfer coefficient k_0 between the bulk liquid and the pores:

$$\frac{1}{k_{0,p}} = \frac{1}{k_{ext}} + \frac{R}{5D_e} \quad (14)$$

$$\frac{1}{k_{0,mp}} = \frac{1}{k_{ext}} + \frac{R}{5D_s} \quad (15)$$

Where $k_{o,p}$ and $k_{o,mp}$ are the overall transfer coefficient for macro- and meso-pores and for micropores respectively (m s^{-1}).

With these assumptions, the final form of the model becomes:

$$\varepsilon_p \frac{d\overline{C}_p}{dt} + \sigma_p \rho \frac{d\overline{Q}_p}{dt} = a_s k_{o,p} (C - \overline{C_p}) \quad (16)$$

$$\frac{d\overline{Q}_p}{dt} = K_e \frac{d\overline{C}_p}{dt} \quad (17)$$

$$\frac{d\overline{Q}_{mp}}{dt} = \frac{a_s k_{o,mp}}{\sigma_{mp}\rho} (C - \overline{C_{mp}^e}) \quad (18)$$

$$\overline{C}_{mp}^e = \frac{\overline{Q}_{mp}}{K_e} \quad (19)$$

$$\frac{dQ_{ext}}{dt} = \frac{a_s k_{ext}}{\sigma_{ext}\rho} (C - C_{ext}^e) \quad (20)$$

$$C_{ext}^e = \frac{Q_{ext}}{K_e} \quad (21)$$

$$\frac{dC}{dt} = \frac{\varepsilon - 1}{\varepsilon} [a_s k_{o,p} (C - \overline{C_p}) + a_s k_{o,mp} (C - \overline{C_{mp}^e}) + a_s k_{ext} (C - C_{ext}^e)] \quad (22)$$

The overscored concentrations $\overline{C}$ and $\overline{Q}$ represent concentrations averaged over the particle with respect to the radial coordinate and hence depend only on the time coordinate. The total adsorbed quantity Q (g g^{-1}) results from a mass balance calculation over the different particle compartments:

$$Q = \sigma_p \overline{Q}_p + \sigma_{mp} \overline{Q}_{mp} + \sigma_{ext} Q_{ext} + \varepsilon_p \frac{S}{\rho} \overline{C}_p \quad (23)$$

The model contains a set of parameters available from experimental data and measurements, listed with their values in Table 2.

The system of equations (Eq.16-22) was numerically resolved in MATLAB®. A multi-parameter optimisation procedure was used for fitting the four specific parameters, i.e. K_e, $k_{o,p}$, $k_{o,mp}$ and k_{ext}, based on the objective function OF to be minimized:

$$OF = \frac{1}{n} \sum_{1}^{n} \left(\frac{\left| C_{sim} - C_{exp} \right|}{C_{exp}} \right)^2 \quad (24)$$

where n is the number of experimental data, and C_{sim} and C_{exp} are the simulated and measured bulk concentrations respectively.

The model should represent the adsorption process for any initial conditions (adsorption and desorption processes) and contact durations. The complete sets of adsorption experimental data (i.e. kinetics and pseudo-isotherm results) were used for the fitting procedure: about 100 and 70 points for toluene and naphthalene respectively. Desorption experimental data were then used for model validation.

The model presents the advantages of considering different kinds of pores with their transport specificities and using mean concentrations of a given compartment, thus simplifying the numerical resolution. The principal weakness is that the porous system is considered to be built up only of parallel pores while, in reality, connections also exist between pores. Ding et al. (2002) used a model based on two types of interconnected porosity. This model is more realistic but its numerical resolution is not trivial (partial differential equations of second order with complex boundary

conditions). Its use for common applications and extensions for adsorber design could be very difficult.

4. Results and discussion

As explained previously, two kinds of experiments were performed: (1) a kinetic study in which the evolution of the eluate concentration was measured versus time; (2) a pseudo-isotherm study in which the evolution of the eluate concentration was measured when the ratio GAC/liquid (i.e. S/L) varied, for a given initial concentration $C_{0,exp}$ and a given constant contact time. Examples of experimental results are given in Figure 2 for toluene and naphthalene: kinetics obtained for different initial concentration values ($C_{0,exp}$) and isotherms obtained for different $C_{0,exp}$ and contact times.

The experimental results show the dependence of the adsorption kinetics and isotherms on the initial concentration. The explanation of the experimental results is not obvious especially for the atypical behaviour of the isotherms. A tentative application of commonly used isotherm models like those of Langmuir or Freundlich was unsuccessful because the fitted constants were found to be dependent on the concentration domain. The commonly used kinetic models (first or second order) are unable to correctly describe the shape of the kinetic curves on the whole time scale and exhibit a dependence on the concentration domain.

The fact that the isotherms apparently depend on the initial concentration and on the contact time demonstrates that the experimental system was not at equilibrium and this was decisive for the development and application of the conceptual model

379 presented. So, the term “pseudo-isotherm” is more suitable than “isotherm” and will
380 be used hereafter.
381 The modelling results and the experimental data are represented in Figure 2 for the
382 kinetic study (Figures 2.a and 2.c) and for the pseudo-isotherms (Figures 2.b and
383 2.d). The model represents the experimental data in a satisfactory manner.
384 Table 3 shows the values of the adjusted parameters by molecule. It is important to
385 note that only one set of parameters for each molecule allows the model to correctly
386 predict the overall data obtained in different conditions.
387
388 The relevance of the adjusted values of the parameters was assessed through their
389 physical significance.
390 The constant K_e, having the units of $m^3\ m^{-2}$, is not comparable with other adsorption
391 constant values (in L kg^{-1}) presented in the literature because of the different
392 adsorption models applied and the hypotheses concerning the equilibrium state.
393 The effective diffusion coefficients (shown in Table 3) for the two types of pores
394 considered in the model were calculated using the formula of Eq.14 and Eq.15. The
395 values are reasonable for the type of porosity and diffusion mechanism considered.
396 For reference, the molecular diffusion coefficients in water are $9.5*10^{-10} m^2\ s^{-1}$ and
397 $6.6*10^{-10} m^2\ s^{-1}$ for toluene and naphthalene respectively.
398 Finally, the k_{ext} value corresponds to typical values for liquid transfer around solid
399 particles in stirred liquids, which are commonly between 10^{-6} and $10^{-4} m\ s^{-1}$.
400
401 The adsorption in a non-homogenous porous matrix is a sequential process in terms
402 of mass transfer and sorbate distribution among the different compartments. If,
403 during the first moments, it is essentially the external surface that is occupied by the

404 sorbate, the prolonged contact time favours a redistribution of the molecules over the
405 different compartments driven by the concentration gradient. This phenomenon
406 depends on the diffusion coefficients and slows down the attainment of an
407 equilibrium state.
408
409 The curves in Figures 3.a and 3.b were obtained by simulation using the
410 experimental conditions of the kinetic study in the case of naphthalene
411 (C_0 = 22g m^{-3}, S/L=0.04g L^{-1}) and using the fitted values of the model parameters (as
412 listed in Table 3). For comparison, a simulation was also made with S/L=4g L^{-1} and is
413 represented by the grey lines in Figure 3.a.
414 Figure 3.b shows the total quantity adsorbed Q (Eq.23) and the distribution of the
415 sorbent among the different compartments of the GAC particles as calculated by the
416 model: on the external surface ($\sigma_{ext} Q_{ext}$), adsorbed on macro- and meso-pore
417 surfaces ($\sigma_p \overline{Q}_p$), retained in macro- and meso-pore liquid ($V_p \overline{C}_p$), adsorbed in
418 micropores ($\sigma_{mp} \overline{Q}_{mp}$).
419
420 Two kinetic domains can be distinguished at different time scales: firstly a short
421 period of several hours corresponding to a massive adsorption on the external
422 surface, followed by a steep decrease in the bulk concentration due to macropore
423 adsorption. A pseudo-equilibrium state is observed after about 100h
424 (for S/L=0.04g L^{-1}) when the bulk concentration seems to be stabilised but, in fact, a
425 slow increase in the micropore adsorption still occurs. A significant evolution of the
426 macroscopic parameters (bulk concentration) would be observed only at very long
427 time periods due to the very slow diffusion in the micropores. The influence of solid to
428 liquid ratio on the macroscopic behaviour of the adsorption process is significant, the

pseudo-equilibrium state being more rapidly attained for high S/L (grey curves in Fig 3.a). The model used here considers that the different types of pores are independent (parallel), i.e. the micropores and macropores do not communicate inside the porous system but communicate directly with the bulk liquid. This is an "optimistic" model because the concentration gradient for microporous diffusion is at its maximum (in non-equilibrium adsorption, the bulk liquid is always more concentrated than that in the macropores). The simulations show that, even with this optimistic hypothesis, molecules like PAH in aqueous solutions are mostly adsorbed in the macro- and meso-porosity (for short time periods) and thus the use of microporous GAC is not necessary.

Among the adjusted parameters, the adsorption constant, K_e, and the mass transfer coefficient for macro- and meso-pores $k_{o,p}$ (or the effective diffusion coefficient D_e) are the most sensitive. Figure 4.a shows a sensitivity study carried out for the kinetic curve of naphthalene. Each curve was calculated by multiplying the parameters K_e, D_e, D_s and k_{ext} by 10, one by one. The sensitivity of a given parameter is not the same over the whole time scale and this result was expected.

The effective diffusion coefficient affects the first period when meso- and macro-pore adsorption takes place. An increase in the adsorption coefficient results in a slowing down of the adsorption kinetics (Valderrama et al., 2008b) and, obviously, in another equilibrium (pseudo-equilibrium) state. The least sensitive parameter is the solid diffusion coefficient and this is explained by a low adsorption in the micropores, at least for the time scale studied. The external mass transfer parameter is not sensitive either; k_{ext} for liquid films in stirred systems takes values between 10^{-4} and 10^{-6}m s^{-1} (Roustan, 2003) and, in this range, the simulations are within the experimental data domain. The GAC used in industrial applications has narrow size dispersion so the

particle radius should not be a sensitive parameter for a given GAC type. Calculations made with 2R and R/2 gave the same sensitivity results as k_{ext} (in formula 14 and 15 it is obvious that the diffusion coefficient makes the major contribution to the overall transport).

The model was then confronted with desorption experiments (naphthalene) in order to validate it and to evaluate its predictive performance. The complex experimental protocol composed of an adsorption step followed by two successive desorption steps was simulated using the previously adjusted parameters. As Figure 4.b shows, the simulation results are in agreement with the experimental values.

5. Conclusions

The experimental study of the adsorption/desorption process in various operating conditions and the modelling and simulation work lead to the conclusions drawn below.

1) The adsorption/desorption of aromatic compounds in aqueous solutions on GAC is a complex process which cannot be represented by simple and usual kinetic models (pseudo-first-order, second order, intraparticle diffusion or Elovich) over a wide range of initial concentrations and time periods. These models are not predictive because the equations and parameters contained in them lack physical meaning.

2) Pseudo-equilibrium states were observed on kinetic curves after about twenty hours of contact. Experimental isotherms determined with different initial concentrations and for different contact times clearly show that reaching the equilibrium state requires hundreds of hours.

3) A multi-compartment dynamic model allowed the deconvolution of the experimentally observed curves and explains the occurrence of many kinetic domains. These kinetic domains are related to the GAC structure and correspond to the different dynamic processes: on the particle surface, in the macro-meso pores and in the micropores. It was expected a priori and then demonstrated by modelling that, at short times, the external surface adsorbs the major part of the solute, then a redistribution of the adsorbed quantity takes place by migration inside the macro-meso pores and then in the micropores, tending towards an equilibrium state in the long term.

4) Concerning the structure of the model, a set of four parameters characterising the solute-sorbent interaction (linear adsorption constant and transport parameters) are necessary and cannot be obtained by direct measurements. These parameters are evaluated by fitting the model on a set of experimental data. Once the set of four parameters has been determined, the model becomes predictive for the molecule-GAC pair, being able to simulate the sorption (adsorption-desorption) process in different conditions of concentrations (large range of $C_{0,exp}$), liquid/solid ratios, contact times, initial conditions, etc. This is what was demonstrated by the successful simulation of successive adsorption-desorption experiments in the case of naphthalene.

5) The modelling and simulation results confirm the experimental observations and show that, for short time periods, the major adsorbed quantity is located on the external surface and in the macro-meso pores. This conclusion is important for further process design, for the choice of the GAC according to its porous structure and in relation with the process contact time.

6) The model takes into account the dominant phenomena occurring in the system studied and the specific properties of the adsorbent related to the porous system, being sufficiently complete to describe this kind of system. The principal weakness lies in the parallel pore assumption, the main consequence of which could be a slight overestimate of the microporous adsorption (supposition not verified). However, in the case of the system studied (PAH in aqueous solution adsorbed on GAC), the microporous adsorption is still very low and hardly useful for a real application. Consequently, the model presented is considered well suited to modelling adsorption/desorption processes for aqueous PAH solutions on GAC.

7) Besides its predictive character, the model is mathematically simple and easy to solve, and hence it can be easily used in more complex models describing treatment processes and coupled bio-physico-chemical phenomena or it can be used with different adsorption equilibrium laws (non-linear in this case).

6. Acknowledgements

The authors thank Evrard Mengelle and Gérard Cancel for their technical support. This work was partly supported by the research agency of the French government (ANR). Activated carbon characterization was performed in Ecole des Mines Albi, centre RAPSODEE, campus Jarlard, F-81013 Albi, France.

References

Water Framework Directive 2000. Directive 2000/60/EC of the European Parliament and of Council of 23 October 2000 establishing a framework for community action in the field of water policy. Official Journal of the European Communities, p. 1–72.

Ania, C.O., Cabal, B., Pevida, C., Arenillas, A., Parra, J.B., Rubiera, F., Pis, J.J., 2007. Effects of activated carbon properties on the adsorption of naphthalene from aqueous solutions. Applied Surface Science 253, 5741.

Bouchez, D., Vittorioso, P., Courtial, B., Camilleri, C., 1996. Kanamycin rescue: A simple technique for the recovery of T-DNA flanking sequences. Plant Molecular Biology Reporter 14, 115-123.

Cabal, B., Ania, C.O., Parra, J.B., Pis, J.J., 2009a. Kinetics of naphthalene adsorption on an activated carbon: Comparison between aqueous and organic media. Chemosphere 76, 433-438.

Cabal, B., Budinova, T., Ania, C.O., Tsyntsarski, B., Parra, J.B., Petrova, B., 2009b. Adsorption of naphthalene from aqueous solution on activated carbons obtained from bean pods. Journal of Hazardous Materials 161, 1150-1156.

Cheremisinoff, N.P., Cheremisinoff, P.N., 1993. Carbon adsorption for pollution control.

Chien, S.H., Clayton, W.R., 1980. Application of Elovich Equation to the Kinetics of Phosphate Release and Sorption in Soils. Soil Sci Soc Am J 44, 265-268.

Cooney, D.O., Xi, Z.P., 1994. Activated Carbon Catalyzes Reactions of Phenolics during Liquid-Phase Adsorption. Aiche Journal 40, 361-364.

Cornelissen, G., Gustafsson, Ouml, 2005. Predictions of large variations in biota to sediment accumulation factors due to concentration dependent black carbon adsorption of planar hydrophobic organic compounds; Environmental Toxicology and Chemistry 24, 495-498.

Crittenden, J.C., Hand, D.W., Arora, H., Lykins, B.W., 1987. Design Considerations for Gac Treatment of Organic-Chemicals. Journal American Water Works Association 79, 74-82.

Derylo-Marczewska, A., M. Jaroniec, D. Gelbin and A. Seidel, 1984. Heterogeneity effects in single-solute adsorption from dilute solutions on solids. Chem. Scr 24, 239-246.

Ding, L.P., Bhatia, S.K., Liu, F., 2002. Kinetics of adsorption on activated carbon: application of heterogeneous vacancy solution theory. Chemical Engineering Science, 57, 3909-3928

Do, D.D., Rice, R.G., 1986. Validity of the Parabolic Profile Assumption in Adsorption Studies. Aiche Journal 32, 149-154.

Douben, 2003. PAHs: An Ecotoxicological Perspective. Ecological and Environmental Toxicology Series. P.E.T. Douben.

562 **Gleuckauf, J.I.C.a.E., 1947. The influence of incomplete equilibrium on the front**
563 **boundary of chromatograms and the effectiveness of separation. J Chem Soc, 1315–**
564 **1321.**

565 **Goto, M., Smith, J.M., Mccoy, B.J., 1990. Parabolic Profile Approximation (Linear**
566 **Driving-Force Model) for Chemical-Reactions. Chemical Engineering Science 45, 443-**
567 **448.**

568 **Huang, C.W., Hung, Y.T., Lo, H.H., 1988. Contact Oxidation Process Followed by**
569 **Activated Carbon Adsorption for Textile Waste-Water Treatment. Acta Hydrochimica**
570 **Et Hydrobiologica 16, 593-605.**

571 **Jonker, M.T.O., Koelmans, A.A., 2002. Extraction of polycyclic aromatic hydrocarbons**
572 **from soot and sediment: Solvent evaluation and implications for sorption mechanism.**
573 **Environmental Science & Technology 36, 4107-4113.**

574 **Lagergren, 1898. Zur theorie der sogenannten adsorption gelöster stoffe. K. Sven 24, 1-**
575 **39.**

576 **Liu, Y., Shen, L., 2008. From Langmuir Kinetics to First- and Second-Order Rate**
577 **Equations for Adsorption. Langmuir 24, 11625.**

578 **Pikaar, I., Koelmans, A.A., van Noort, P.C.M., 2006. Sorption of organic compounds to**
579 **activated carbons. Evaluation of isotherm models. Chemosphere 65, 2343-2351.**

580 **Roustan, M., 2003. Transfert gaz-liquide dans les procédés de traitement des eaux et des**
581 **effluents gazeux, Lavoisier, 798p.**

582 **Seidel, A., Tzscheutschler, E., Radeke, K.-H., Gelbin, D., 1985. Adsorption equilibria of**
583 **aqueous phenol and indol solutions on activated carbons. Chemical Engineering Science**
584 **40, 215.**

585 **Seredych, M.M., Gun'ko, V.M., Gierak, A., 2005. Structural and energetic**
586 **heterogeneities and adsorptive properties of synthetic carbon adsorbents. Applied**
587 **Surface Science 242, 154.**

588 **Srivastava, S.K., Tyagi, R., 1995. Competitive adsorption of substituted phenols by**
589 **activated carbon developed from the fertilizer waste slurry. Water Research 29, 483.**

590 **Summers, R.S., Roberts, P.V., 1988. Activated Carbon Adsorption of Humic**
591 **Substances.1. Heterodisperse Mixtures and Desorption. Journal of Colloid and Interface**
592 **Science 122, 367-381.**

593 **Valderrama, C., Cortina, J.L., Farran, A., Gamisans, X., Heras, F.X.D.L., 2008a.**
594 **Kinetic study of acid red "dye" removal by activated carbon and hyper-cross-linked**
595 **polymeric sorbents Macronet Hypersol MN200 and MN300. Reactive & Functional**
596 **Polymers 68, 718-731.**

597 **Valderrama, C., Cortina, J.L., Farran, A., Gamisans, X., Lao, C., 2007. Kinetics of**
598 **sorption of polyaromatic hydrocarbons onto granular activated carbon and Macronet**
599 **hyper-cross-linked polymers (MN200). Journal of Colloid and Interface Science 310, 35-**
600 **46.**

Valderrama, C., Gamisans, X., de las Heras, X., Farran, A., Cortina, J.L., 2008b. Sorption kinetics of polycyclic aromatic hydrocarbons removal using granular activated carbon: Intraparticle diffusion coefficients. Journal of Hazardous Materials 157, 386-396.

Vinod, V.P., Anirudhan, T.S., 2003. Adsorption Behaviour of Basic Dyes on the Humic Acid Immobilized Pillared Clay. Water, Air, & Soil Pollution 150, 193.

Weber, W.J.J., J.C. Morris, 1963. Kinetics of adsorption on carbon from solution. J. Sanit. Eng. Div. 89, 31-60.

WHO, 2006. Guidelines for Drinking water Quality. World Health Organization Press, Switzerland.

Williams, P.T., 1990. Sampling and Analysis of Polycyclic Aromatic-Compounds from Combustions Systems - a Review. Journal of the Institute of Energy 63, 22-30.

Wu, F.C., Tseng, R.L., Huang,S.C., Juang, R.S., 2009. Characteristics of pseudo-second-order kinetic model for liquid-phase adsorption: A mini-review. Chemical Engineering Journal

Zimmerman, J.R., Ghosh, U., Millward, R.N., Bridges, T.S., Luthy, R.G., 2004. Addition of Carbon Sorbents to Reduce PCB and PAH Bioavailability in Marine Sediments: Physicochemical Tests. Environmental Science & Technology 38, 5458.

Figure captions

Figure 1.a: Scanning electron micrographs of the activated carbon PICAS35; b) scheme of a GAC particle

Figure 2.a: Adsorption kinetics of toluene at 25°C, (♦)$C_{0,exp}$=5g m^{-3} (▲)$C_{0,exp}$=13g m^{-3}

Figure 2.b: Adsorption pseudo-isotherms of toluene at 25°C (●)$C_{0,exp}$=21g m^{-3} /contact time=600h, (♦)200g m^{-3} /94 h, (■)10g m^{-3} / 48h ,(▲)7g m^{-3} / 48h.

Figure 2.c: Adsorption kinetics of naphthalene at 25°C, (▲)$C_{0,exp}$=20g m^{-3}.

Figure 2.d: Adsorption pseudo-isotherms of naphthalene at 25°C (●)$C_{0,exp}$=6g m^{-3} /contact time=48h, (▲)30g m^{-3} / 144h.

Figure 3.a: Simulation of adsorption behaviour: (a) Naphthalene concentration (g m^{-3}) in liquid compartments with two different Solid/Liquid ratios: S/L=0.04g L^{-1} (black lines) and S/L=4g L^{-1} (grey lines) with C_0 = 22g m^{-3}.

*Figure 3.*b: Naphthalene distribution between the particle compartments with C_0 = 22g m^{-3} and S/L=0.04g L^{-1}.

Figure 4.a: Sensitivity analysis on adsorption kinetics of naphthalene ($C_{0,exp}$=20g m^{-3}). Experimental data (♦) and simulated data (black line), effect of K_e, D_e, D_s and k_{ext}.

Figure 4.b: Pseudo-isotherms of adsorption and desorption of naphthalene at 25°C (●) adsorption experimental data $C_{0,exp}$=6g m^{-3} /contact time =48h; (♦)first desorption; (□)second desorption; simulated data are represented in line.

Table captions

Table 1: Model variables

Table 2: Parameters available from experimental data and measurements

Table 3: Parameters estimated by model fitting procedure and estimated diffusion coefficients

650

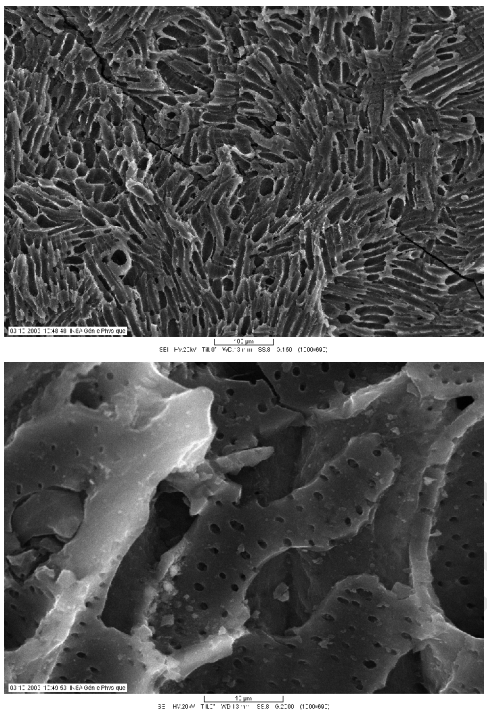

1.a

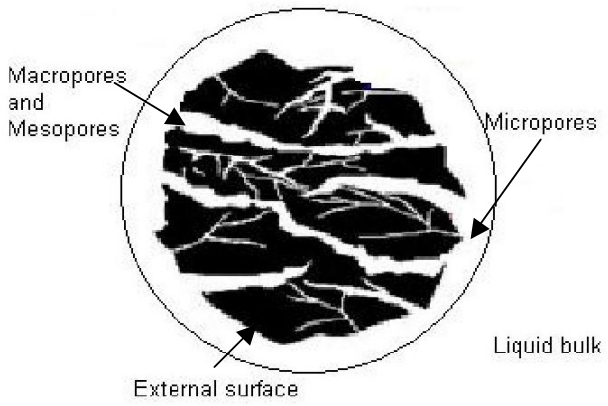

1.b

651 *Figure 1*

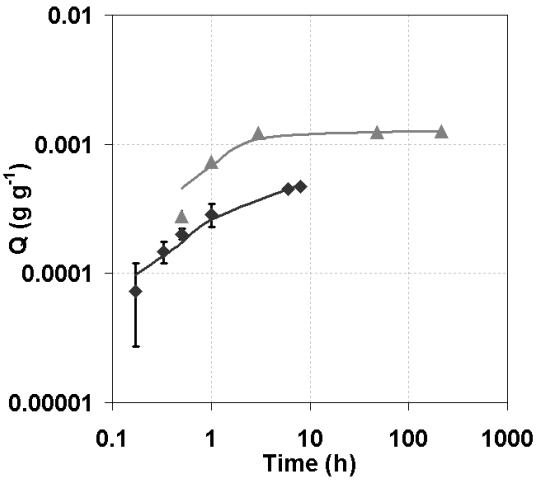

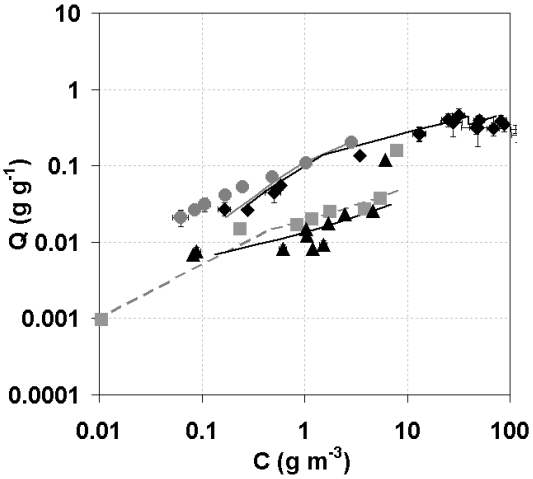

2.a

2.b

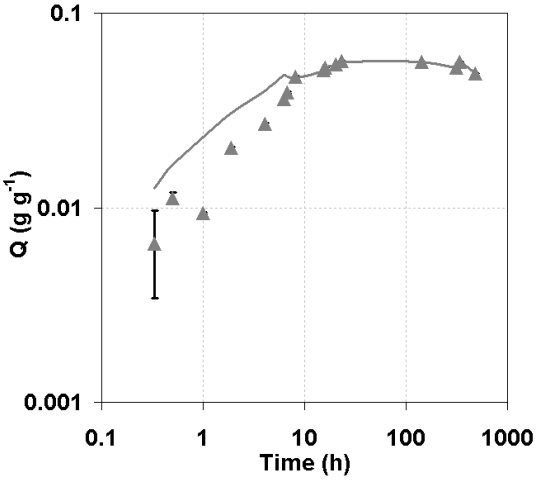

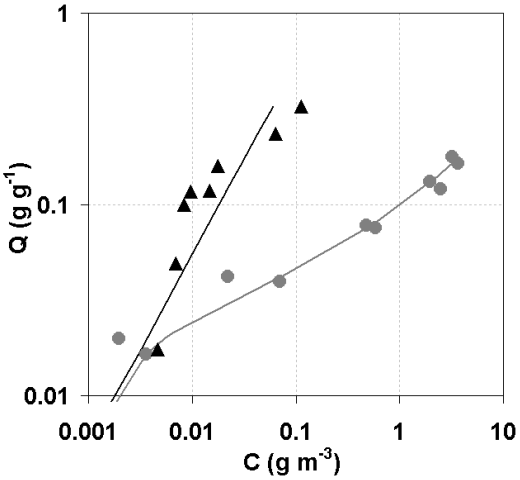

2.c

2.d

652 Figure 2
653

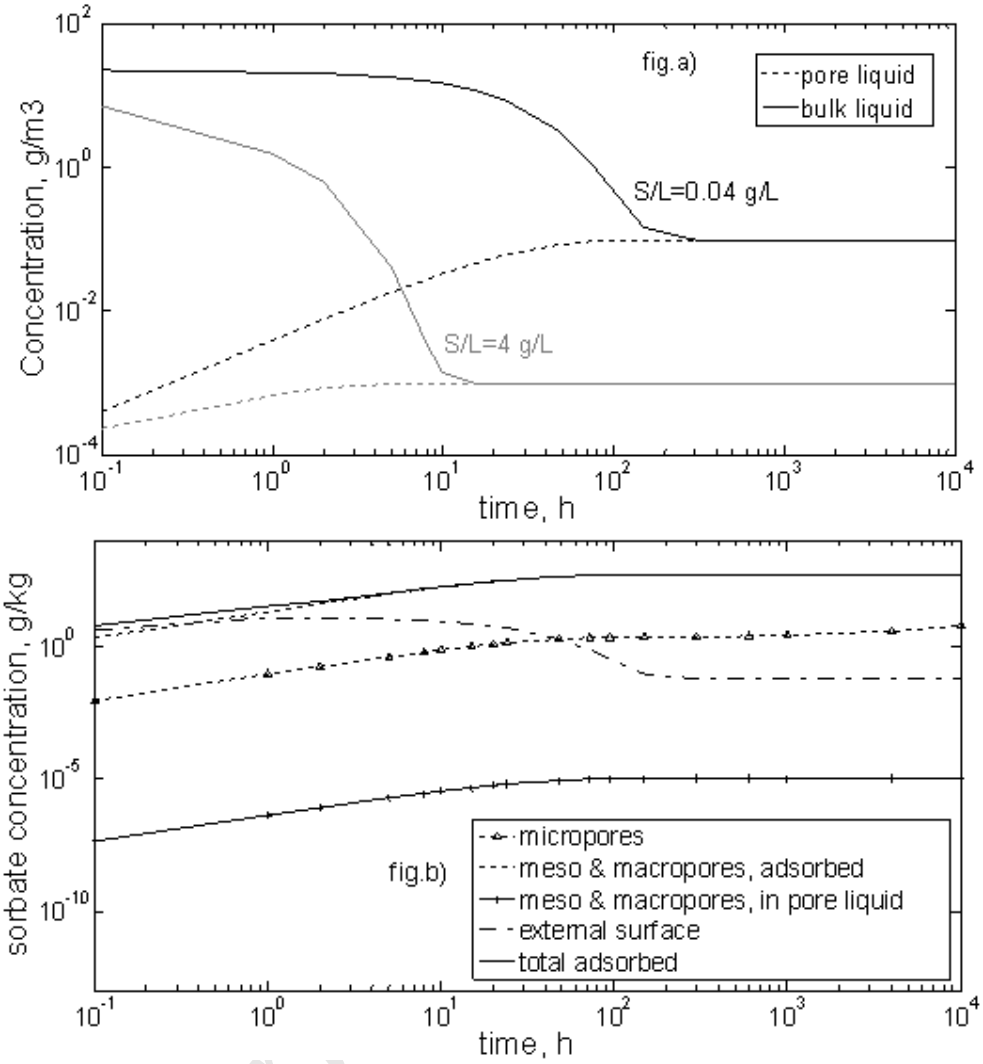

Figure 3.

656

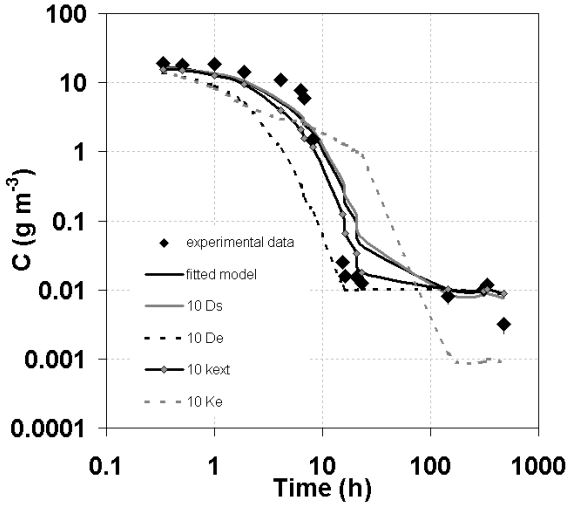

4.a

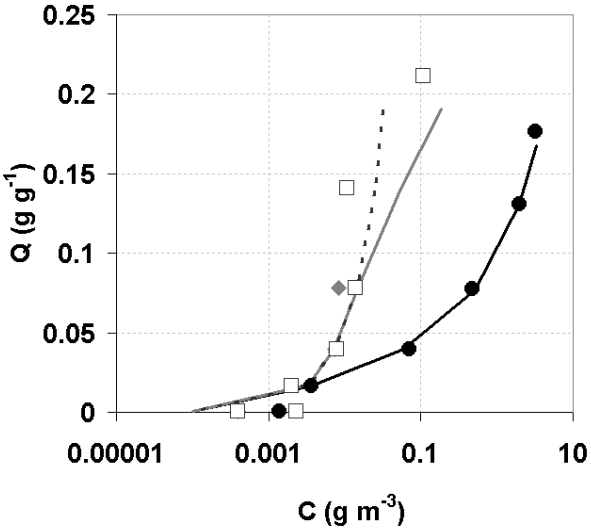

4.b

657 Figure 4

658

658 Table 1*:* Model variables

Variable	Description	Unit
C	Concentration in the bulk liquid	g m^{-3}
C_{ext}^{e}	Equilibrium concentration close to the external surface	g m^{-3}
C_{p}	Concentration in the mesopores and macropores	g m^{-3}
$\overline{C}_{p}$	Mean concentration in the mesopores and macropores	g m^{-3}
C_{mp}^{e}	Equilibrium concentration in the liquid phase at the micropore inlet	g m^{-3}
$\overline{C}_{mp}^{e}$	Equilibrium mean concentration in the liquid phase at the micropore inlet	g m^{-3}
Q	Total quantity adsorbed	g g^{-1}
Q_{ext}	Quantity adsorbed on the particle external surface	g m^{-2}
Q_{p}	Quantity adsorbed in the mesopores and macropores	g m^{-2}
$\overline{Q}_{p}$	Mean quantity adsorbed in the mesopores and macropores	g m^{-2}
Q_{mp}	Quantity adsorbed in the micropores	g m^{-2}
$\overline{Q}_{mp}$	Mean content in the micropores	g m^{-2}
r	Radial direction	m
t	Time	s

659

659 *Table 2*: Parameters available from experimental data and measurements

Parameter	Description	Unit	Experimental value or estimation
a_s	Specific surface area of GAC particles	$m^2\ m^{-3}$	$a_s=f_a\ (3/R)$; a_s = 39340
f_a	Shape factor	-	4.3; estimated by microscope imaging (Figure 1.a)
$C_{0,exp}$	Concentration of the pollutant solution used for adsorption (desorption) experiments	$g\ m^{-3}$	Different experimental values
C_{exp}	Final concentration in an experimental sample	$g\ m^{-3}$	Different experimental values
V	Volume of liquid in the experimental sample	m^3	Different experimental values
R	Particle mean radius	m	$3.25\ 10^{-4}$ (manufacturer data)
S	GAC mass in the experiments	g	Different experimental values
V_p	Volume of mesopores and macropores	$m^3\ g^{-1}$	$1.1\ 10^{-7}$ (BET evaluation)
ρ	GAC particle density	$g\ m^{-3}$	420000 (manufacturer's data)
ε	Bulk liquid volume fraction		$\varepsilon = \frac{V}{(V + S/\rho)}$
ε_p	Mesopore- and macropore porosity		$\varepsilon_p = \rho\ V_p$
σ_p	Mesopore and macropore specific surface area	$m^2\ g^{-1}$	394 (BET evaluation)
σ_{mp}	Micropore specific surface area	$m^2\ g^{-1}$	1576.6 (BET evaluation)
σ_{ext}	External surface specific area available for adsorption	$m^2\ g^{-1}$	$\sigma_{ext} = 0.5(a_s/\rho)$

660

660 *Table 3:* Parameters estimated by model fitting procedure and estimated diffusion
661 coefficients
662

Parameter	Description	Unit	Toluene	Naphthalene
K_e	Adsorption equilibrium constant	m	$2.3\ 10^{-4}$	$1.38\ 10^{-2}$
$k_{o,p}$	Mesopore/macropore overall mass transfer coefficient	$m\ s^{-1}$	$1.9\ 10^{-7}$	$2.2\ 10^{-6}$
$k_{o,mp}$	Micropore overall mass transfer coefficient	$m\ s^{-1}$	$1.9\ 10^{-8}$	$1.9\ 10^{-8}$
k_{ext}	External mass transfer coefficient	$m\ s^{-1}$	$1.0\ 10^{-5}$	$7.0\ 10^{-6}$
D_e	Effective mesopore/macropore pore diffusion coefficient	$m^2\ s^{-1}$	$1.3\ 10^{-11}$	$2.1\ 10^{-10}$
D_s	Effective surface diffusion coefficient	$m^2\ s^{-1}$	$1.2\ 10^{-12}$	$1.2\ 10^{-12}$

663